PRELIMINARY MEASUREMENTS AND PERFORMANCE ASSESSMENT ON A SMALL VIRC

Abstract. This report describes the measurements and a first general assessment of the small VIRC. The experiments were carried out with the scope of characterizing some important parameters of the empty chamber (viz. without an EUT) such as the first resonant frequencies, the resonant frequency variation, the stirring ratio, the power deviation to the mean the VSWR and the Q factor. A preliminary discussion about the effect on the VIRC performance of some factors involved in the stirring method are addressed. These experiments helped me also as a first approximation to the VIRC, in order to gain more understanding and confidence in its use. More tests can be done in the future to experiment more thorough means of characterizing the VIRC, specially for testing SMILE.

1. Test setup

- **Screened enclosure**. Fabric used: Kassel Copper-Silver SHIELDEX Fabric. Joined using sewing. Internal dimensions (tight): 1.5 m × 1.2 m × 1 m (height). Volume (tight): 1.8 m^3. One access panel, originally thought to hold the samples for shielding effectiveness measurements in the dual VIRC configuration. Holding structure.
- **TX/RX Antennas**. Two monopoles of 7 cm were used as the transmitting and receiving antennas. The antennas were directly plugged to feed-through SMA connectors in the panel's handle holes. The distance from the wall to the antennas was more than 13 cm.
- **Spectrum Analyzer**. A Rohde & Schwarz FSL spectrum analyzer (f=9 kHz ... 18 GHz) was used. The tracking generator featured in this instrument was used to analyze the signals inside the VIRC.

2. Electromagnetic Modes inside the Cavity

The cavity was excited by means of a continuous wave signal delivered to the transmitting antenna by means of the tracking generator. Figure 1 shows the power in dBm measured by the receiving antenna as a function of the frequency of excitation. No correction due to the antenna factors or losses in the cables were done.

The vertical lines indicate the position (in frequency) where a resonant mode is present according to the theoretical calculation. As we can see, some measured peaks correspond approximately to the calculated theoretical frequencies of resonance. Nevertheless, it is also observed that there are many existing peaks that do not correspond to any calculated eigenfrequency, and on the other hand, some eigenfrequencies that do not correspond to any measured peak. This effect is mainly due to the fact that the theoretical calculation assumes a perfectly rectangular cavity, which is something practically impossible to achieve with the VIRC, even with

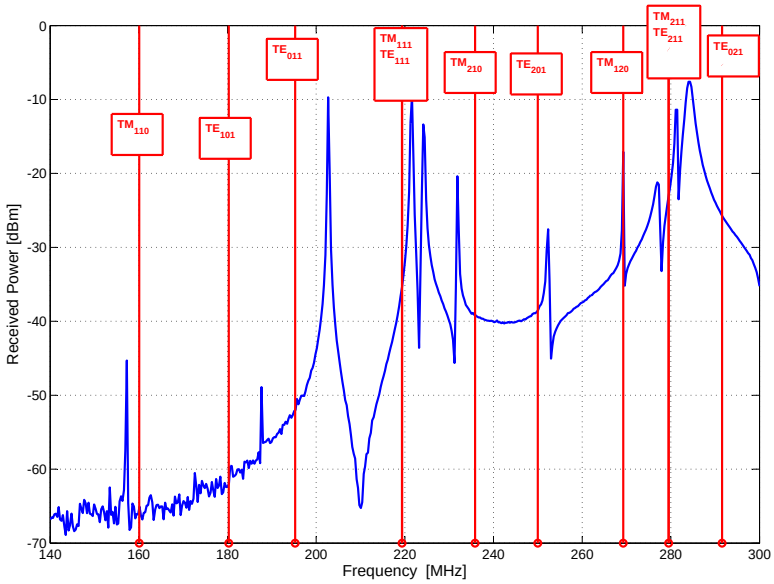

FIGURE 1. Received power inside the cavity. The red vertical lines show the theoretical resonant modes of a rectangular cavity with the same dimensions.

the corners at maximum tightness. Nevertheless, there's a quite satisfactory correspondence, specially in the number of modes present in this lower part of the frequency band. It can also be observed how intrinsically degenerate modes as the TM and TE with no index equal to zero are "split" in the VIRC, improving the modal density (i.e. TM_{111} and TE_{111} and TM_{211} and TE_{211}).

3. Resonance frequency variation (Δf)

The change in resonance frequency provides an indication of the stirring efficiency. Figure 2 shows the influence in the modal structure when different configurations of the VIRC's wall are assumed. Each measurement was performed with a steady chamber, thus in static conditions. We can see that even for low frequencies (below the possible LUF), the stirring method consisting on moving the walls does change the resonance frequencies. Nevertheless, these changes are still largely correlated for the first resonances.

Generally this is the way Δf is characterized, that is just by observation of either the power or the field strength as function of the frequency for several fixed boundary conditions. It is clear that this indicator can not be measured at high frequencies, since mode overlapping would make impossible to distinguish from a resonance to another. On the other hand, there are still neither theoretical developments nor empirical guidelines to use this indicator to characterize a particular RC. Normally it is used as a quick reference for comparing two stirring methods.

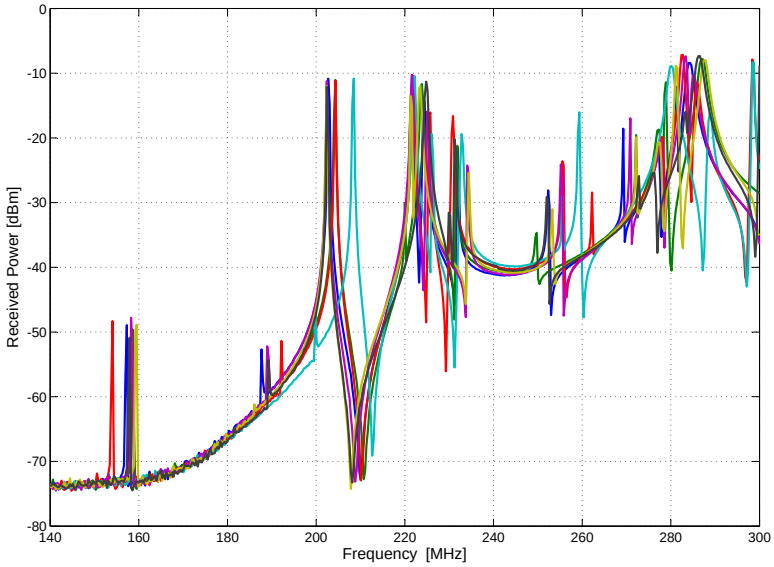

FIGURE 2. Power received by an antenna inside the small VIRC at a frequency sweep from 140 MHz to 300 MHz for six different configurations of the chamber. The influence of the stirring in the modal structure can be appreciated.

As far as my personal experience is concerned, the Δf for the small VIRC largely outperforms other similar measurements in "conventional" reverberation chambers.

4. Power Deviation to the Mean and Stirring Ratio

The maximum received power in a well performing reverberation chamber is approximately 7 to 10 dB greater than the average received power, regardless of the chamber type or location. This difference is known as the power deviation to the mean and it can be analytically derived using the conventional statistical models for reverberation chambers. The 7 to 10 dB maximum power to the mean ratio corresponds to typical data samples ranging from 100 to 10000.

It is also known that the maximum received power is almost always at least 20 dB greater than the minimum received power. This difference (known as maximum-to-minimum ratio, paddle- (or tuner-) effectiveness, or stirring ratio) indicates that changes in the boundary conditions resulted in significant changes in the EME close to the receiving antenna. This is therefore another indication that the stirring method is satisfactory. The minimum difference of 20 dB was recommended and stands as a parameter of the stirring performance although no theoretical justification was ever given. Usually, the stirring ratio is taken to be the best measured data ratio indicator.

Figure 3 shows the minimum, average, and maximum received power measured in the small VIRC.

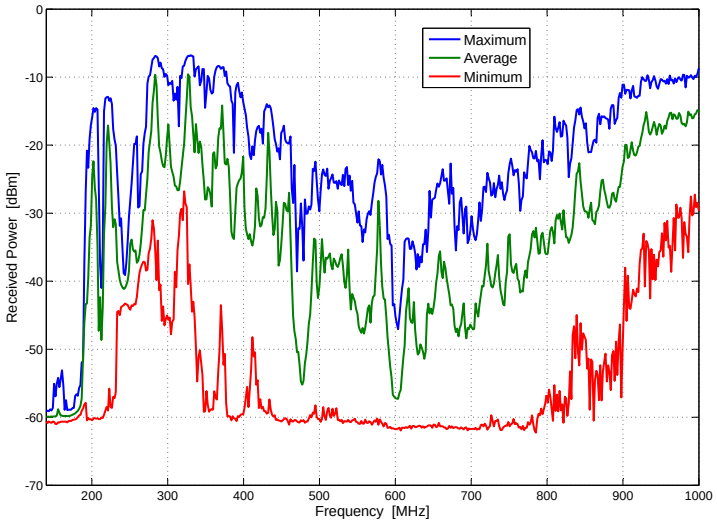

FIGURE 3. Measured minimum, average and maximum received power as a function of the frequency in the small VIRC.

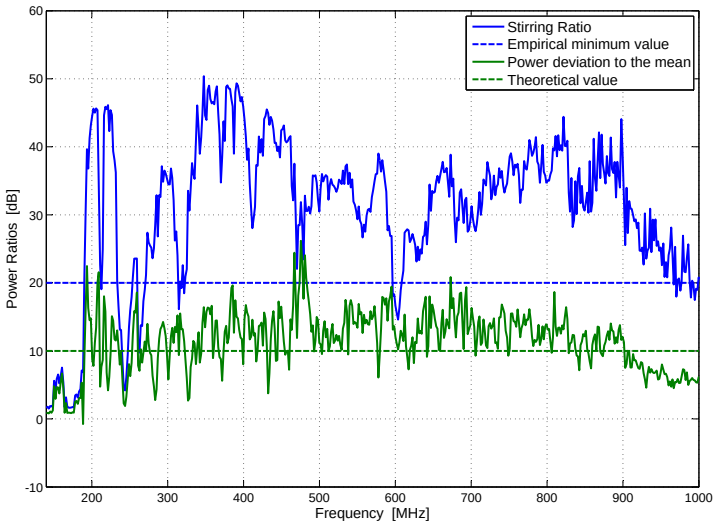

FIGURE 4. Power deviation to the mean and stirring ratio values as a function of the frequency in the small VIRC.

Figure 4 shows the power deviation to the mean with its expected theoretical value and the stirring ratio.

5. Voltage Standing Wave Ratio (VSWR)

Another interesting parameter is the VSWR, which indicates at what frequency the maximum energy transfer can be achieved. Given measurements of the reflected power of the antennas (normally forward reflection, that is at the transmitting antenna), the VSWR can be calculated at each stirrer position:

$$VSWR = \frac{1 + \sqrt{P_{refl}}}{1 - \sqrt{P_{refl}}}. \tag{1}$$

Since (1) is calculated for different stir states, we can compute the minimum, average and maximum VSWR. Figure 5 shows the maximum and minimum VSWR for forward reflected power in the small VIRC. The VSWR was measured by means of the Rohde & Schwarz SWR Bridge ZRB2. It is clear that the VSWR measurement is antenna-dependent. Plots of the VSWR of the antennas are included sometimes simply to indicate the characteristics of the antennas when placed inside a RC. The actual values of the VSWR are not used in any calculation.

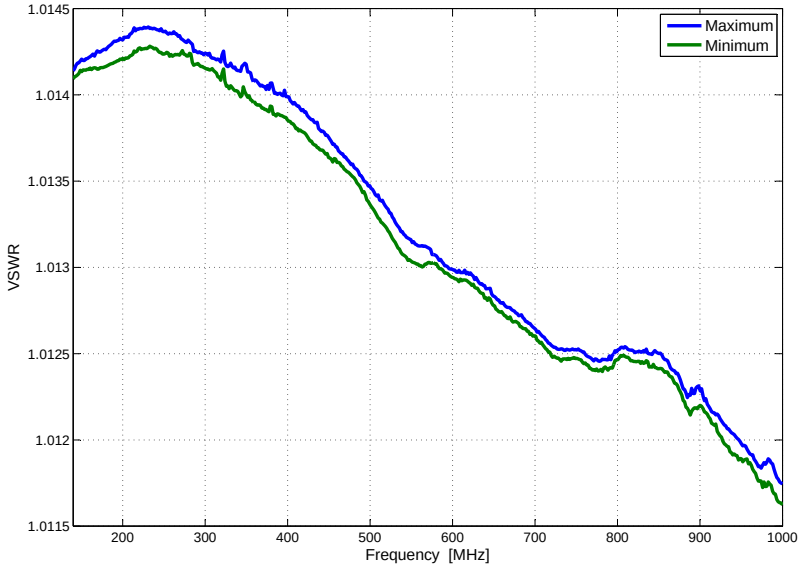

Figure 5. Minimum and maximum VSWR measured in the small VIRC for reflected transmitting (forward) power of a monopole antenna.

6. Autocorrelation

The autocorrelation coefficient can be calculated in the VIRC by measuring a set of samples at a given frequency obtained while moving the walls, and then

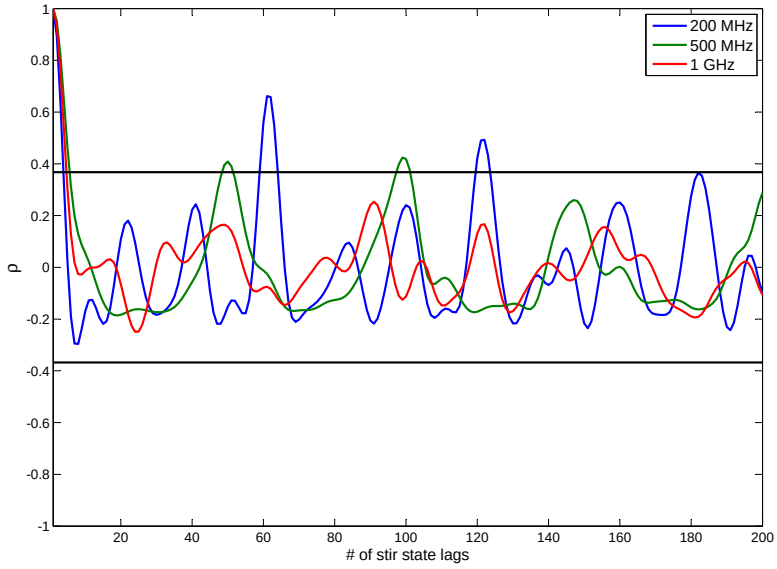

FIGURE 6. Small VIRC stirring efficiency measurements based on the power received by an antenna P_{RX} for three different frequencies at the same spatial position. The horizontal lines define the uncorrelated region $|\rho| \leq \frac{1}{e}$

.

calculating the correlation between the original set and the same set but shifted in r sample steps. Mathematically:

$$\rho(r) = \frac{1}{N} \frac{\sum_{i=1}^{N} (x_i - \langle x \rangle)(x_{i+r} - \langle x \rangle)}{s_x^2}, \tag{2}$$

where N is the total number of samples and $x_1, x_2, x_3, \ldots x_N$ is the field magnitude of interest (x), s_x^2 is the sample variance estimator and $\langle x \rangle$ the mean value. The subindex $i + r$ is *modulo* N. It is defined in practice that $|\rho| \leq \frac{1}{e} \approx 0.37$ are the values of ρ that would indicate fairly reasonable uncorrelation.

Autocorrelation coefficient measurements are shown in Fig. 6, where the small VIRC stirring efficiency measurements based on the power received by an antenna P_{RX} for three different frequencies at the same spatial position are shown. At each frequency, 400 samples were taken.

7. Q MEASUREMENTS

The quality factor has also been considered to characterize the cavity. Each of the many distinct modes inside the cavity carries it own Q-value. We omit the explicit expressions here for the sake of brevity. The present section includes a

discussion about two different methods for measuring the Q-factor, i.e. the transmission method and the decrement method, and several measured Q-factors in the frequency band f = 200 ... 1000 MHz. It has to be emphasized that the measurements performed at this stage were done with the chamber in a still position, thus without any stirring process. That is the reason why the Q measurements methods used are not the ones normally used in RCs.

7.1. **The Q_{110}^{TM} Measurement.** The first mode chosen for the present study was the TM_{110} (the fundamental resonant mode). Figure 7 shows the resonance curve of this mode. The relation between the resonant frequency f and the 3dB bandwidth Δf gives the measured value of the Q_{110}^{TM} factor by the transmission method.

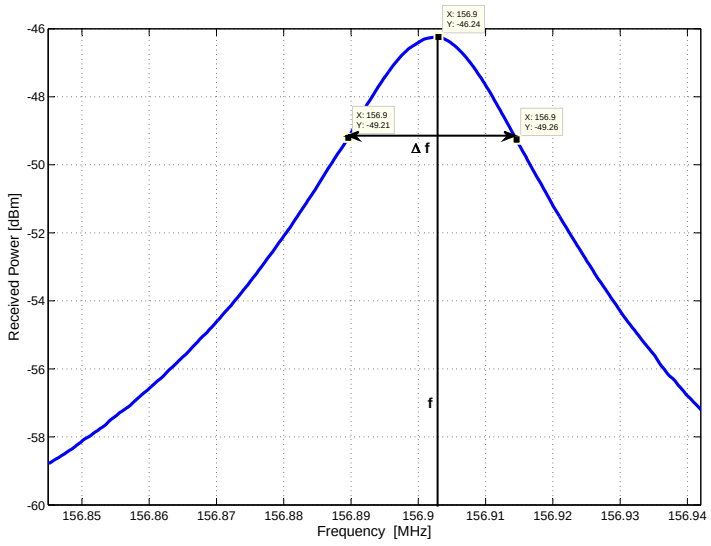

FIGURE 7. Resonance curve of the TM_{110} mode used to calculate Q_{110}^{TM} via the transmission method. The resulting Q is $Q_{110}^{TM} \approx 6276$.

For the decrement method, the cavity was excited with a pulse modulated sine from the signal generator. The frequency of the sine was that of resonance of the mode under study, f_{110}, the period of the pulse T = 10 ms and a duty-cycle of D = 0.5. The power at the receiving antenna is measured using the zero span mode and a resolution bandwidth RBW = 1 kHz in the spectrum analyzer. Figure 8 shows the trace of the received power when the exciting signal passes from the "on" state to the "off" state. The Q-factor can be extracted by measuring the slope of the region of exponential decay.

The measured Q_{110}^{TM} is 6276 and 88925 for the transmission and decrement method, respectively. The theoretical Q_{110}^{TM} is $\approx$ 900000. It is widely known that although the Q-factor can be calculated theoretically, measured Q values are usually an order of magnitude lower partly due to the imperfections in the construction of the room, losses in cables, connectors, etc. In other words, theoretical

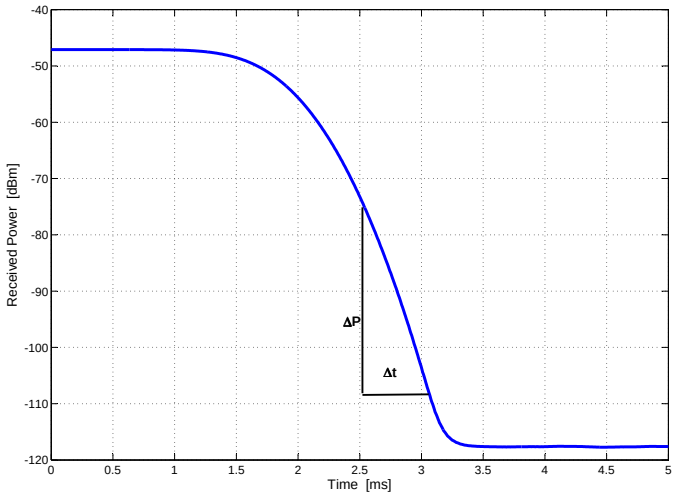

FIGURE 8. Trace of the received power at frequency f_{110}. After the exciting signal is switched off, an exponential decay can be observed. Q_{110}^{TM} can then be extracted via the decrement method. The resulting Q is $Q_{110}^{TM} \approx 88925$.

calculations relate to the intrinsic Q while measurements relate to the external Q (intrinsic + cables, etc).

About the noticeable difference between the transmission and decrement methods, it has to be said that while the transmission method is the simplest measurement of Q, it suffers from the fact that it is largely sensitive to the losses in the coupling system and thus, is not capable of producing accurate results. On the other hand, the decrement method behaves in a more unambiguous manner, rendering it specially convenient for high-Q cavities.

7.2. **Q measurements at frequency band f = 200 ... 1000 MHz.** The decrement method can be applied to any frequency and not exclusively when it coincides with a resonance, as is the case of the transmission method. In this way it was possible to measure the Q-factor at seventeen different frequencies evenly spaced in the band f = 200 ... 1000 MHz. The results are shown in Fig. 9 where also a comparison with the theoretical calculation is shown.

8. Loose Tent

Whether it is more convenient to fix the tent tight or loose could be a matter of concern when assessing the optimum stirring strategy. The results showed so far were found with the VIRC in a tight fashion. For the sake of comparison, we will present some of these measurements, but with a loose chamber.

8.1. **Electromagnetic Modes inside the Cavity.** Figure 10 shows the modal structure when the chamber is fixed in a loose fashion.

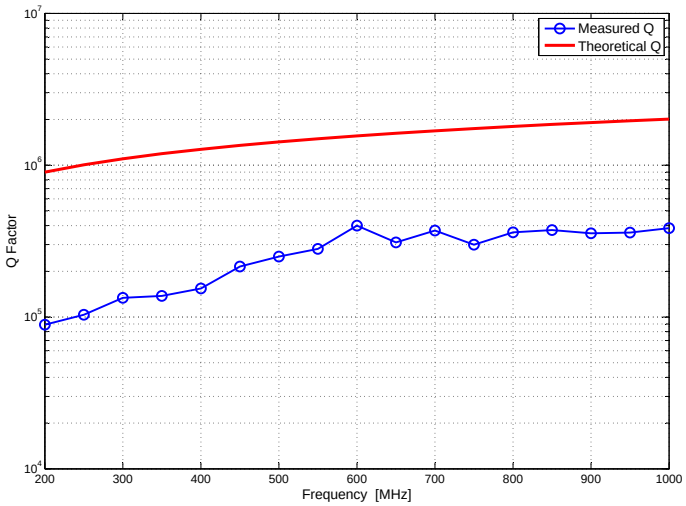

FIGURE 9. Q-factors of the screened cavity: theoretical and measured, in the frequency band f = 200 ... 1000 MHz.

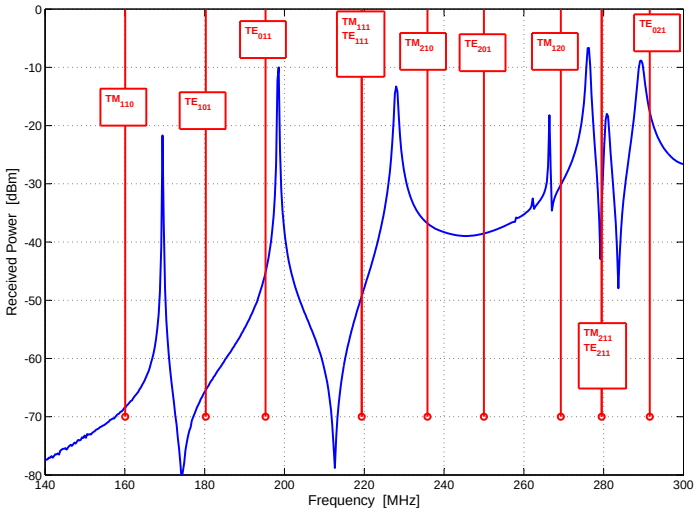

FIGURE 10. Received power inside the loose cavity. The red vertical lines show the theoretical resonant modes of a rectangular cavity with the same inner surface.

Comparing it with Fig. 1, it can be seen the considerable change in the modes distribution. The departure from the theoretical modes of a rectangular chamber

of the same inner surface is also important. It is to be noticed the apparent lack of mode degeneracy and mode overlapping even in the low frequency band. It is also important to point out the lesser number of modes present, when compared to the tight configuration at the same frequency.

8.2. **Resonance frequency variation (Δf).** Figure 11 shows the resonance frequency variation when the chamber is fixed in a loose fashion.

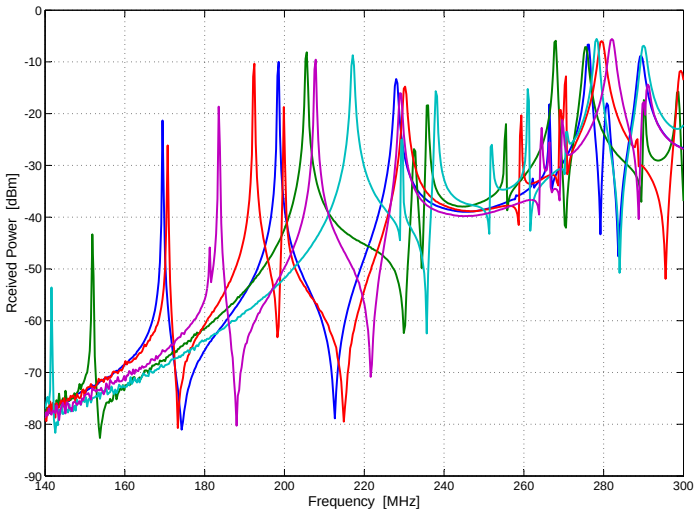

FIGURE 11. Power received by an antenna inside the small VIRC in a loose fashion, for five different configurations of the chamber. The influence of the stirring in the modal structure can be appreciated.

It can be seen a relatively larger Δf when compared to that of Fig. 2. Even though the number of modes in the loose chamber is less than the number of modes in the tight chamber, these modes seem to spread more evenly when they are stirred, better contributing to field uniformity. This is mainly due to the fact that with a loose chamber, a larger number of different configurations can be achieved.

It is to be noticed that even if the total volume of the loose chamber is lower than the total volume of the tight chamber, there exist some modes at surprisingly low frequencies, approximately 151.8 MHz and 141.6 MHz. Therefore, it seems that the smaller volume of the loose configuration should not be a major drawback. Nevertheless, this is something to be further investigated.

8.3. **Power Deviation to the Mean and Stirring Ratio.** Figures 12 and 13 show the minimum, average and maximum received power and the power ratios, respectively, for the loose chamber

Comparison with Figs. 3 and 4 result in a unequivocally outperforming of the loose configuration with respect to the tight one, when assessing the stirring ratio and the power deviation to the mean. Nevertheless, it has to be pointed out that the

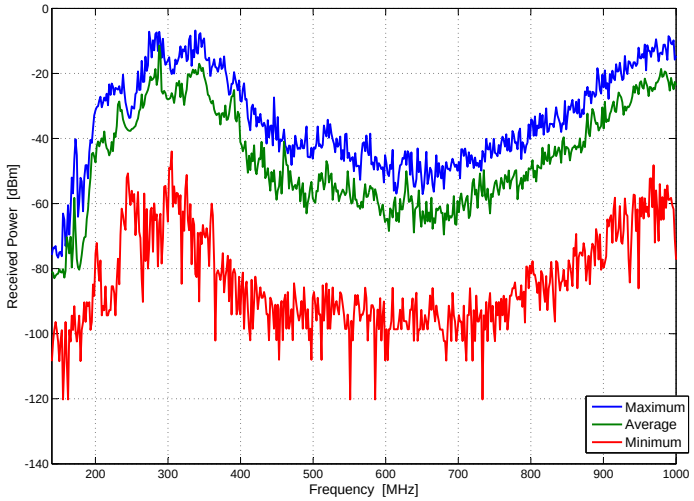

FIGURE 12. Measured minimum, average and maximum received power as a function of frequency for the loose configuration of the small VIRC.

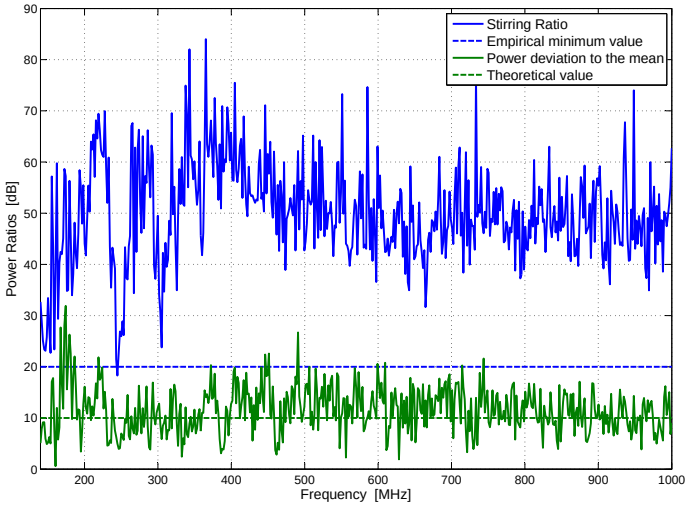

FIGURE 13. Power deviation to the mean and stirring ratio values as a function of frequency for the loose configuration of the small VIRC.

mode stirring with the loose chamber was performed manually, with the possibility

of producing a much larger movement of the walls. In practice, such a stirring method seems largely unpractical.

8.4. **Autocorrelation.** Figure 14 shows the autocorrelation coefficient measurements for the chamber in the loose configuration.

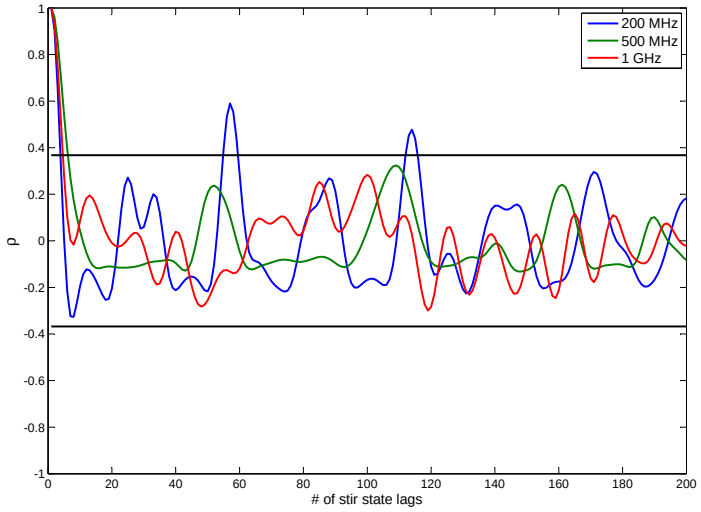

FIGURE 14. Small VIRC stirring efficiency measurements for the loose configuration based on the power received by an antenna P_{RX} for three different frequencies at the same spatial position. The horizontal lines define the uncorrelated region $|\rho| \leq \frac{1}{e}$.

The comparison with Fig. 6 does not provide us with a clear conclusion of whether one configuration outperforms the other one or viceversa.

9. CONCLUSIONS

An empty cavity characterization was performed, helping in learning about the principal resonant modes of the cavity and the influence of moving the walls in the resonant structure for two chamber configurations: tight and loose. Two methods for measuring the quality factor in resonant cavities were tested.